Coupling multiscale observations to evaluate hyporheic nitrate removal at the reach scale

Coupling multiscale observations to evaluate hyporheic nitrate removal at the reach scale

Jay P. Zarnetske[1,4], Roy Haggerty[2,5], and Steven M. Wondzell[3,6]

[1]Department of Geological Sciences, Michigan State University, East Lansing, Michigan 48824 USA

[2]College of Earth, Ocean, and Atmospheric Sciences; and Institute for Water and Watersheds, Oregon State University, Corvallis, Oregon 97331 USA

[3]Pacific Northwest Research Station, Corvallis Forestry Sciences Laboratory, Corvallis, Oregon 97331 USA

Abstract: Excess NO_3^- in streams is a growing and persistent problem for both inland and coastal ecosystems, and denitrification is the primary removal process for NO_3^-. Hyporheic zones can have high denitrification potentials, but their role in reach- and network-scale NO_3^- removal is unknown because it is difficult to estimate. We used independent and complementary multiscale measurements of denitrification and total NO_3^- uptake to quantify the role of hyporheic NO_3^- removal in a 303-m reach of a 3rd-order agricultural stream in western Oregon, USA. We characterized the reach-scale NO_3^- dynamics with steady-state ^{15}N-NO_3^- tracer-addition experiments and solute-transport modeling, and measured the hyporheic conditions via in-situ biogeochemical and groundwater modeling. We also developed a method to link these independent multiscale measurements. Hyporheic NO_3^- removal (rate coefficient λ_{HZ} = 0.007/h) accounted for 17% of the observed total reach NO_3^- uptake and 32% of the reach denitrification estimated from the ^{15}N experiments. The primary limitations on hyporheic denitrification at the reach scale were availability of labile dissolved organic C and the restricted size of the hyporheic zone caused by anthropogenic channelization (sediment thickness ≤1.5 m). Linking multiscale methods made estimates possible for hyporheic influence on stream NO_3^- dynamics. However, it also demonstrated that the traditional reach-scale tracer experimental designs and subsequent transport modeling cannot be used alone to directly investigate the role of the hyporheic zone on reach-scale water and solute dynamics.

Key words: surface-water–groundwater interaction, denitrification, nutrient cycling, nitrogen, residence time

Anthropogenic alterations to global bioavailable N budgets, landscape use, and hydrologic cycles have resulted in excess NO_3^- in many aquatic ecosystems (Seitzinger et al. 2006, Gruber and Galloway 2008). These excess NO_3^- stream loads can degrade down-gradient freshwater and coastal systems (e.g., Sala et al. 2000, Smith 2003, Diaz and Rosenberg 2008). Thus, we need to understand and manage the sources and sinks of NO_3^- in stream ecosystems (Boyer et al. 2006). Streams have many sources of NO_3^- (e.g., fertilizer runoff, wastewater discharge, organic N mineralization). Processes, such as uptake and subsequent burial in sediment, may remove NO_3^- from stream water, but only denitrification permanently transfers N from the stream to the atmosphere (Seitzinger et al. 2006). Denitrification occurs in many locations in stream ecosystems, but the hyporheic zone (HZ) is a known hotspot for denitrification because it has strong physical transport and

biological reaction gradients, which in turn, promote redox gradients and denitrification (Duff and Triska 2000). However, the role of hyporheic denitrification at the reach scale is rarely accounted for in nutrient-cycling studies. Thus, whether hyporheic denitrification is responsible for a substantial amount of the NO_3^- removal at the reach and network scale is not known.

Methods for measuring and modeling hyporheic and reach NO_3^- removal and denitrification are difficult to implement and result in high uncertainty (Groffman et al. 2006, Birgand et al. 2007, Böhlke et al. 2009). A key barrier to evaluating the role of hyporheic NO_3^- removal at larger scales is that hyporheic studies tend to be done at spatial scales that are much smaller than the length of the reach and time scales that are much longer than the residence time of water flowing through the surface channel. Therefore, the scientific techniques developed to measure

hyporheic processes and stream-reach processes are very different.

Reach-scale NO_3^--removal investigations are conducted primarily via NO_3^- addition and tracer experiments (e.g., Stream Solute Workshop 1990, Mulholland et al. 2004). In these studies, nutrient concentration dynamics are observed along the experimental reach or at the end of the reach. The reach concentration observations are then used to model and infer coupled hydrologic and biological processes affecting transport of the nutrients. These nutrient-addition experiments are capable of measuring the integrated effects of hydrologic and biological process controls on N uptake in streams (e.g., Peterson et al. 2001, Mulholland et al. 2004). In addition, development of the stream nutrient-spiraling concept for NO_3^- and other nutrients (Webster and Patten 1979, Newbold et al. 1981) provided a unifying conceptual model for how an element (e.g., N or P) is transported and cycled in a stream ecosystem via coupled hydrologic and biological pathways. The uptake length (S_w) is the average channel distance a molecule travels before being taken up by a physical or biological retention or removal process. S_w is used to compare nutrient processing between widely varying stream systems (e.g., Mulholland et al. 2008). However, the fact that S_w integrates both hydrologic and biological processes means that it cannot be used to isolate individual hydrologic or biological processes controlling NO_3^- dynamics. For example, it cannot distinguish the role of net denitrification on the observed S_w or where in the stream NO_3^- uptake is occurring. The use of ^{15}N-NO_3^- (hereafter $^{15}NO_3^-$) helped to overcome some of the limitations of S_w because tiny amounts of labeled N could be traced through the different compartments of a stream ecosystem (Mulholland et al. 2004). Despite the advances in many stream-tracer techniques since the Stream Solute Workshop (1990), reach-scale experiments and resulting metrics, including S_w, still cannot be used to determine whether observed NO_3^- removal occurred in the main channel or in the HZ.

An alternative to the reach-scale methods described above is to use networks of wells installed in the HZ to measure NO_3^- dynamics directly in the HZ (e.g., Valett et al. 1996, Hedin et al. 1998, Baker et al. 1999). However, calculating rates of denitrification in the HZ is then complicated by problems of calculating the flux of water through the HZ, primarily because of unknown subsurface heterogeneity. Furthermore, direct measurements can be difficult because of very long transport time scales.

Multiscale measurements made in the HZ and the stream must be integrated to evaluate the role of hyporheic NO_3^- removal at the reach scale effectively (Marzadri et al. 2012, Harvey et al. 2013). Therefore, we linked independent and complementary measurements and models of hyporheic and reach-scale dynamics to quantify the role of hyporheic denitrification on NO_3^- uptake in an experimental reach of an upland agricultural stream. We used a highly instrumented gravel bar to make multiple in-situ biogeochemical measurements under near ambient NO_3^- (i.e., <3% above background) and natural hydraulic conditions. We characterized the hydrologic conditions of the gravel bar with tracer studies and groundwater flow modeling. We estimated reach-scale NO_3^- dynamics via a $^{15}NO_3^-$-addition experiment (sensu the 2nd Lotic Intersite Nitrogen eXperiment [LINX2]; Mulholland et al. 2004). We used the $^{15}NO_3^-$ study to quantify reach-scale total NO_3^- uptake and denitrification rates, which we then related directly to the hyporheic NO_3^- denitrification and transport rates.

METHODS
Study site

The study site was a 303-m reach (Fig. 1A) of Drift Creek, a 3rd-order stream in the Willamette River basin in western Oregon, USA (lat 44.9753°N, long 122.8259°W). The catchment up-gradient of the study site is 65.17 km^2 and consists of mixed land uses with primarily agriculture and residences served by septic systems. Annual precipitation (~1190 mm) comes mostly as rain during the winter months (November–March). After the winter rainy season ends, base flow gradually decreases to an annual minimum in early September.

The experimental reach was modified in the past by channelization. The modified reach has a slope of 0.0071 m/m, and the active channel is predominantly pool–riffle with alluvium consisting of poorly sorted sand, gravel, cobbles, and boulders. The stream is channelized into competent bedrock and separated from the flood plain. The alluvium above the bedrock surface is limited to a thickness of 0 to ≤1.5 m. This limited alluvium constrains the extent of the HZ in the experimental reach. At the time of the experiment, the stream had a mean water depth of 0.33 m, mean wetted width of 5.21 m, and mean discharge of 22.0 L/s, which increased by 1.2% over the study reach because of lateral inflows (Zarnetske et al. 2011a).

The hyporheic-zone study site was described by Zarnetske et al. (2011a, b). It is an ~6.1 × 4-m lateral gravel bar with a riffle on the south side and a bedrock outcrop on the north side (Fig. 1B). The head drop from the head of the gravel bar to the pool below was 0.19 m during the study. This head loss induces lateral hyporheic flow paths that originate at the head of the gravel bar and terminate in the down-gradient pool (Zarnetske et al. 2011a). The alluvial thickness at the gravel-bar site is 1.2 ± 0.25 m. This gravel bar has a well network consisting of eleven 3.8-cm-diameter wells screened from 0.2 to 0.4 m below ground surface.

The stream and hyporheic background biogeochemical conditions (Table 1) permitted $^{15}NO_3^-$ enrichment of NO_3^- for 27.5 h, which was sufficient to create steady-state (i.e.,
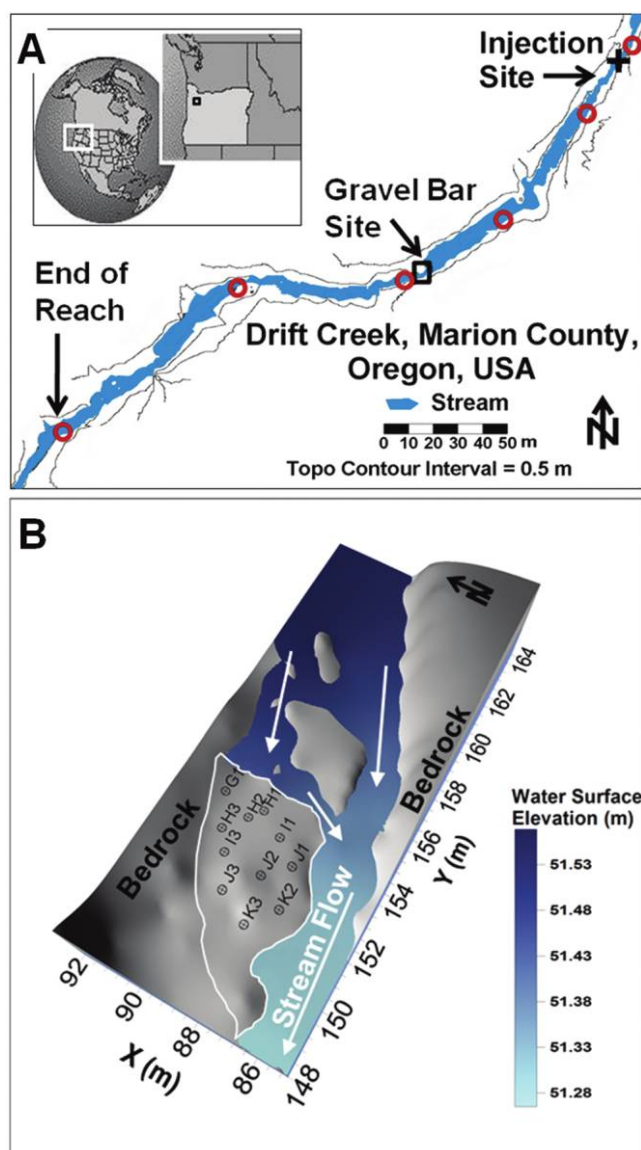
Figure 1. Drift Creek experimental reach (A) and instrumented gravel-bar site (B). The open circles in panel A are the longitudinal sampling locations for the whole-reach experiment, and the circles with cross-hairs in panel B are the hyporheic well locations. The white polygon on the gravel-bar site represents the spatial domain of the hyporheic exchange model.

plateau) values in all measured solute reservoirs in the experimental reach and instrumented HZ.

Field experimental procedures

The field and laboratory procedures used to collect the data for our study were presented in detail by Zarnetske et al. (2011a), and are briefly summarized below. We performed a whole-stream steady-state $^{15}NO_3^-$ and conservative tracer (Cl$^-$) injection during summer baseflow conditions (23–24 August 2007). We used methods adapted from Mulholland et al. (2004), and released an injection solution of $^{15}NO_3^-$ (as 99% enriched K$^{15}NO_3$) and Cl$^-$ (as NaCl) at a constant rate into a riffle at the head of the reach for 27.5 h. We estimated the K$^{15}NO_3$ addition rate based on targets of $\delta^{15}N$ enrichment of 10,000‰ in the stream water $^{15}NO_3^-$ and <3% increase in ambient NO_3^- concentration (36.6 g ^{15}N added to stream over duration of experiment). The Cl$^-$ mass-addition target was to elevate the background stream Cl$^-$ 400% and to generate a 50% increase above ambient specific conductivity (SC). We injected the solution into a turbulent riffle sufficiently upstream of the 1st sampling location to ensure compete lateral and vertical channel mixing at all downstream sampling locations (Fig. 1A).

We used SC to measure Cl$^-$ transport through the stream and HZ. We collected SC measurements in all 11 gravel-bar wells and in the stream water at the head and base of the gravel bar every 60 s, which was sufficient to capture the details of the Cl$^-$ breakthrough curves. We used these SC measurements as input data for stream and hyporheic solute-transport models that quantified transport conditions, including advection rates, residence-time characteristics, and mass-exchange rates between the stream mobile and transient storage zones, including the HZ.

The sampling regime consisted of collecting multiple rounds of stream and hyporheic water samples during the pre-injection (background) and steady-state (plateau) phases of the experiment. We sampled repeatedly during the pre-injection ($n = 3$) and plateau ($n = 5$) periods at each hyporheic-zone location (11 wells and stream water at the gravel-bar head). The plateau sampling period was started 22.5 h after injection started, which is when all hyporheic wells demonstrated near steady-state SC. We collected repeated hyporheic and stream samples approximately every 1 h during the plateau period. In addition, we collected 6 longitudinal samples in duplicate for each sampling period at locations 4 m above and 22, 84, 110, 183, and 303 m below the injection site so that reach-scale NO_3^- uptake and denitrification parameters could be calculated following Mulholland et al. (2004). We analyzed all water samples for key solute concentrations and $\delta^{15}N$ enrichments relevant to the respiratory denitrification process ($^{15}NO_3^-$, $^{15}N_2$). Laboratory procedures for the stream and hyporheic NO_3^-, Cl$^-$, and ^{15}N content of the stream and hyporheic water NO_3^- and N_2 were presented by Zarnetske et al. (2011a).

Immediately after the experiment and during similar stable baseflow conditions, we collected detailed thalweg surface water and channel surface topography data for the reach with a Topcon total station (Model GTS-226; Topcon, Livermore, California) and standard surveying methods with spatial accuracy of $x \leq 1$ m, $y \leq 1$ m, $z \leq 0.01$ m for the 303-m reach and $x \leq 0.1$ m, $y \leq 0.1$ m, $z \leq 0.005$ m for the instrumented gravel-bar site. In addition, we based hydraulic conductivities (K) for the gravel-bar HZ on the geometric mean value of 22 slug tests (2 tests/

Table 1. Mean (±1 SE, *n* = 3) values of background stream and hyporheic biogeochemistry variables with measured median residence time of surface water to each hyporheic well. DO = dissolved O_2, DOC = dissolved organic C, $SUVA_{254}$ = Specific Ultraviolet Absorbance at 254 nm.

Site	Median travel time (h)	DO (mg O_2/L)	NO_3^- (mg N/L)	NH_3 (mg N/L)	DOC (mg C/L)	$SUVA_{254}$ (L mg^{-1} C m^{-1})
Stream	NA	8.31 ± 0.43	0.32 ± 0.01	0.02 ± 0.02	3.01 ± 0.15	3.22 ± 0.18
G1	6.87	2.07 ± 0.05	0.54 ± 0.06	0.11 ± 0.02	2.07 ± 0.15	1.88 ± 0.17
H1	3.80	3.27 ± 0.09	0.43 ± 0.05	0.05 ± 0.01	2.18 ± 0.14	1.25 ± 0.17
H2	16.20	1.30 ± 0.03	0.27 ± 0.03	0.06 ± 0.01	2.10 ± 0.17	1.96 ± 0.21
H3	16.32	0.72 ± 0.06	0.33 ± 0.03	0.05 ± 0.01	2.01 ± 0.20	1.20 ± 0.23
I1	14.90	1.09 ± 0.05	0.25 ± 0.04	0.08 ± 0.01	1.94 ± 0.15	1.79 ± 0.15
I3	18.17	0.93 ± 0.09	0.13 ± 0.00	0.07 ± 0.01	1.98 ± 0.10	1.31 ± 0.11
J1	28.45	0.70 ± 0.06	0.07 ± 0.02	0.01 ± 0.01	1.66 ± 0.12	0.94 ± 0.13
J2	18.95	0.61 ± 0.09	0.13 ± 0.01	0.02 ± 0.01	1.79 ± 0.10	1.27 ± 0.11
J3	21.40	0.65 ± 0.05	0.08 ± 0.01	0.04 ± 0.01	1.71 ± 0.06	1.01 ± 0.07
K2	21.03	0.65 ± 0.05	0.08 ± 0.01	0.04 ± 0.01	1.71 ± 0.06	1.01 ± 0.07
K3	22.70	0.59 ± 0.10	0.09 ± 0.01	0.02 ± 0.01	1.70 ± 0.11	1.05 ± 0.12

well) analyzed with the Bouwer and Rice method (Bouwer and Rice 1976). These survey and *K* data were used to parameterize the numerical groundwater flow model to simulate hyporheic exchange across the gravel-bar site so that total water and NO_3^- flux could be calculated based upon the experimental and model results.

Reach parameter calculations

Reach NO_3^- conditions   We estimated reach NO_3^- uptake and denitrification conditions by following the $^{15}NO_3^-$ tracer experiment and modeling methods of Mulholland et al. (2004), which are summarized here. At longitudinal sampling stations along the reach (Fig. 1A), we calculated specific discharge from the dilution of the Cl^- tracer during plateau conditions. We used these discharge measurements to calculate the tracer $^{15}NO_3^-$ flux at each station by multiplying the discharge by the background-corrected $^{15}NO_3^-$ concentrations. We then calculated the fractional NO_3^- total uptake rate per unit distance (k_{tot}; /m) from the regression of ln(tracer $^{15}NO_3^-$ flux) vs distance from the ^{15}N-injection station. The negative inverse of the regression slope is S_w for NO_3^- (Newbold et al. 1981). From S_w, we calculated the mass-transfer velocity (V_f) of NO_3^- as the specific discharge (Q/w, where w = wetted width) divided by S_w. The mass of NO_3^- taken up from the water column per unit streambed area and time is the areal uptake (U) of NO_3^- and is the product of V_f and the mean ambient NO_3^- concentration (Stream Solute Workshop 1990, Webster and Valett 2006).

We estimated the fractional denitrification rate per unit length (k_{den}) by an N_2 production-rate model (Mulholland et al. 2004). We fit the model of N_2 production to the longitudinal pattern in the fluxes of tracer ^{15}N as N_2 collected during injection plateau. We calculated the flux of $^{15}N_2$ at each longitudinal station by multiplying back-

ground-corrected $^{15}N_2$ by the specific station *Q*. We generated the reaeration rate of N_2 (0.023/m; k_{ar}) used in the model with the surface-renewal model (Owens 1974). Denitrification rates calculated in this way represent a minimum value because we were unable to account for N_2O production in the estimates (see Zarnetske et al. 2011a). However, denitrification in freshwater sediments is almost entirely N_2 production with $N_2O:N_2$ production ratios generally between <0.001 and <0.05 (Seitzinger and Kroeze 1998, Mulholland et al. 2004, Beaulieu et al. 2011). Thus, $^{15}N_2$ alone is able to characterize the large majority of denitrification in the system.

Reach hydrologic conditions   We used a 1-dimensional (1D) solute-transport model to provide optimized parameters for reach-representative estimates of advection, dispersion, and transient storage for our solute-addition experiment. This 1D solute-transport model (STAMMT-L) was described by Haggerty and Reeves (2002) and Haggerty et al. (2002). We briefly describe the governing equations below and show how they relate to the well known and more commonly used OTIS solute-transport model (Bencala and Walters 1983, Runkel et al. 1998). The STAMMT-L model applies a user-specified residence-time distribution to the general 1D advection–dispersion transport equation. The transport equation for a system that is initially tracer-free with no longitudinal inputs is:

$$\frac{\partial c}{\partial t} = -v\frac{\partial c}{\partial x} + D\frac{\partial^2 c}{\partial x^2} - \beta_{tot}\frac{\partial}{\partial t}\int_0^t c(\tau)g^*(t-\tau)d\tau \quad \text{(Eq. 1)}$$

where v is the mean in-stream advection velocity (m/h), D is the longitudinal dispersion (m^2/h), β_{tot} is the ratio of the mass in the immobile zone to that in the mobile zone at equilibrium, c is the conservative tracer concentration

in the stream (mg/L), and τ is the lag time (h). In the last term of Eq. 1, $g^*(t)$ is convolved with the stream concentration to represent exchange with the transient-storage zone, including the HZ, following an appropriate residence-time distribution. The probability density function that the tracer remains in storage after a time, t, is defined as:

$$g^*(t) = \alpha_2 e^{-\alpha_2 t} \qquad \text{(Eq. 2)}$$

for an exponential residence-time distribution where α_2 is the 1st-order rate coefficient (/h). When using an exponential residence-time distribution, this model is equivalent to the OTIS transient-storage model (Runkel et al. 1998). For readers more familiar with the notation used in OTIS, note that $\alpha = \alpha_2 \times \beta_{tot}$ and $A_s/A = \beta_{tot}$. Transient-storage conditions can be further characterized by the mean storage residence time, $\tau_{stor} = 1/\alpha_2$ (h), which represents the average time that tracer spends in the transient-storage zone.

Parameters were estimated by STAMMT-L with a non-linear least-squares algorithm (Marquardt 1963) that minimized the sum of square errors on the logarithms of the tracer concentrations. For all simulations, we calculated the root mean squared error (RMSE) (Bard 1974) between the observed and simulated data. Optimization runs for the tracer test were completed using the exponential residence-time distribution method, and the simulation that generated the lowest RMSE was accepted as the best model. The model parameters ν, D, β_{tot}, and α_2 were calculated in the optimization process.

Hyporheic parameter calculations

Hyporheic NO$_3^-$ conditions   We used SC breakthrough curves collected during the stream tracer injection to measure the median travel time, where the median travel time occurred when SC equaled ½ the plateau value. We subtracted the median travel time measured in the stream at the head of the gravel bar from the median travel time estimated for each well so that our estimate of travel time to wells reflects only the travel time through the HZ. We then related the measured NO$_3^-$ concentrations to these median residence times, so that NO$_3^-$ removal rates could be calculated.

We assumed that in our hyporheic system, the observed NO$_3^-$ removal dynamics are primarily the result of denitrification as evidenced by the $^{15}N_2$ production seen in the gravel bar during the experiment (Zarnetske et al. 2011a). Therefore, we refer to observed decreases in NO$_3^-$ as apparent denitrification. The apparent 1st-order denitrification rate constant, (/h), can be calculated from the observed steady-state hyporheic NO$_3^-$ concentration profiles as:

$$C_{NO_3} = C_{in}e^{-k_{HZ}t_{med}} \qquad \text{(Eq. 3)}$$

where C_{NO_3} is the concentration of NO$_3^-$ (mg N/L), C_{in} is the input concentration (mg N/L), and t_{med} is the median residence time (/h) of water in the HZ as measured from the conservative tracer (Cl$^-$) breakthrough curve.

Hyporheic hydrologic conditions   We used a groundwater flow model (MODFLOW) to simulate 3-dimensional hyporheic exchange flow (HEF) through the gravel bar and to estimate total water and solute flux. The model domain was defined in space by the gravel bar and sediment thickness surveys and was partitioned into 0.05-m horizontal grid cells. The model had 5 layers generating cells matching the vertical resolution (0.20 m) of the screened well sampling location. The stream was modeled as a spatially variable constant-head boundary condition established by the measured surface-water elevations. For all sediment layers, anisotropy of K was incorporated such that $K_{x,y}$ (horizontal) was an order of magnitude greater than K_z (vertical) (Freeze and Cherry 1979). The assigned K value of 4.7×10^{-5} m/s for the model domain was the geometric mean of 22 variable head tests in the gravel bar following the tracer experiment. Effective porosity was set to 0.30. Groundwater and lateral subsurface inflow or outflow was considered negligible in the groundwater model and was not incorporated into the model design because we found no evidence of either occurring over this segment of the stream reach. The groundwater flow was modeled with a steady-state simulation because stream surface flow did not vary sufficiently across the experiment period to detect a change in the wetted perimeter of the gravel bar. The model solves for the distribution of hydraulic heads within the model domain and, subsequently, the velocities and travel times in the HZ (Kasahara and Wondzell 2003, Wondzell et al. 2009). We parameterized the MODFLOW model with measured values. We did not subsequently calibrate the model to improve the fit between predicted heads and those observed in our well field.

We also used the groundwater flow model to calculate the hyporheic–stream exchange rate, α_{HZ} (/h), mean residence time in the HZ, τ_{HZ} (h), and total HEF (L/h). The residence times in the gravel bar were partitioned into 1-h residence-time intervals, and the HEF, Q_{HEF} (L/h), was calculated for each interval (see Kasahara and Wondzell 2003, Wondzell et al. 2009). τ_{HZ} is the mean of the Q_{HEF} distribution normalized by total HEF, and α_{HZ} is $1/\tau_{HZ}$.

Relating hyporheic and reach NO$_3^-$ dynamics

We combined and scaled-up results of the hyporheic NO$_3^-$ dynamics measured in our gravel bar (~10 m length) with reach-scale results from the transient-storage modeling (STAMMT-L; ~300 m length) and the nutrient-spiraling measurements (S_w; ~300 m length) to evaluate the relative contribution of in-stream vs hyporheic pro-

cesses on whole-reach denitrification. Our general approach was to use the stream spiraling results to characterize whole-reach denitrification. We then estimated the hyporheic denitrification by scaling the observed k_{HZ} measured at the gravel-bar scale by the size of the HZ relative to the size of the stream (i.e., scaling via β_{tot}) and α_{HZ}. The individual steps of this approach are explained in more detail below. However, we point out that different approaches result in measurements made at widely varying temporal and spatial scales, and combining these measurements relies on several critical assumptions: 1) that the stream-spiraling measurements provide a reasonable estimate of the combined effects of both in-stream and hyporheic processes, 2) that k_{HZ} measured in the gravel bar is representative of the mean denitrification rate of the entire HZ within our study reach, and 3) that β_{tot} is representative of the hydrologic exchange occurring in the study reach.

The effective NO_3^- removal rate at the reach scale, λ_{tot} (/h), can be represented as the sum of the NO_3^- removal rate in the surface stream channel and benthic layer, λ_{stream} (/h), and in the HZ, λ_{HZ} (/h) as suggested by Runkel (2007) and Botter et al. (2010):

$$\lambda_{tot} = \lambda_{stream} + \lambda_{HZ} \qquad \text{(Eq. 4)}$$

The studies of Runkel (2007), Botter et al. (2010), and Argerich et al. (2011) also showed that λ_{HZ} can be estimated from the hydrologic transport and solute reaction kinetics. Thus, we calculated λ_{HZ} as:

$$\lambda_{HZ} = \beta_{tot}(k_{HZ}\alpha_{HZ})/(k_{HZ} + \alpha_{HZ}) \qquad \text{(Eq. 5)}$$

where β_{tot} is estimated from the reach-scale solute-transport model and α_{HZ} is estimated from the groundwater transport model. Together, these parameters scale the effect of the HZ size and exchange rates on the reach NO_3^- removal dynamics.

We represent λ_{tot} as:

$$\lambda_{tot} = k_{tot}v \qquad \text{(Eq. 6)}$$

from the reach hydrologic transport and spatially explicit NO_3^- reaction kinetics, where the reach mean velocity, v, is used to transform k_{tot} to a temporally explicit NO_3^- removal rate.

We calculated the in-stream NO_3^- removal rate by difference:

$$\lambda_{stream} = \lambda_{tot} - \lambda_{HZ} \qquad \text{(Eq. 7)}$$

We assumed that λ_{HZ} is primarily the result of hyporheic denitrification as indicated by significant hyporheic N_2 production observed in the Drift Creek HZ

(Zarnetske et al. 2011a). Thus, we also related the λ_{HZ} to the measured reach k_{den} generated from the reach $^{15}N_2$-production model. Similar to λ_{tot}, we calculated the reach denitrification rate, λ_{den}, as:

$$\lambda_{den} = k_{den}v \qquad \text{(Eq. 8)}$$

We related the various removal rates to each other by taking the ratio of λ_{HZ} to λ_{tot} and λ_{den}.

RESULTS
Reach conditions

Stream biogeochemical conditions were stable during the experiment. Stream chemistry was nearly constant during the experiment and reflected the pre-injection conditions (Table 1), whereas water temperature varied by 2.4°C during the injection period (range = 14.1–16.5°C). Measured surface-water nutrient and chemistry conditions during the experiment were NO_3^- (0.318–0.325 mg N/L), NH_3 (0.021–0.024 mg N/L), dissolved organic C (DOC) (2.95–3.45 mg C/L), DO (8.10–8.51 mg O_2/L), and pH (6.65–6.85). Stream flow was relatively uniform during the experiment with a mean flow of 22.0 ± 2.2L/s (SD). This variability in discharge was a result of diel evapotranspiration and agricultural withdrawals, but they did not induce measureable changes in the stage of the stream along the reach.

Transient-storage modeling showed good agreement between the simulated and observed conservative-tracer data (RMSE = 0.02; Fig. 2). The estimated reach transport parameters from the STAMMT-L model were v = 67.7 m/h, D = 13.9 m^2/h, τ_{stor} = 0.49 h, α_2 = 2.03/h, and β_{tot} = 0.17
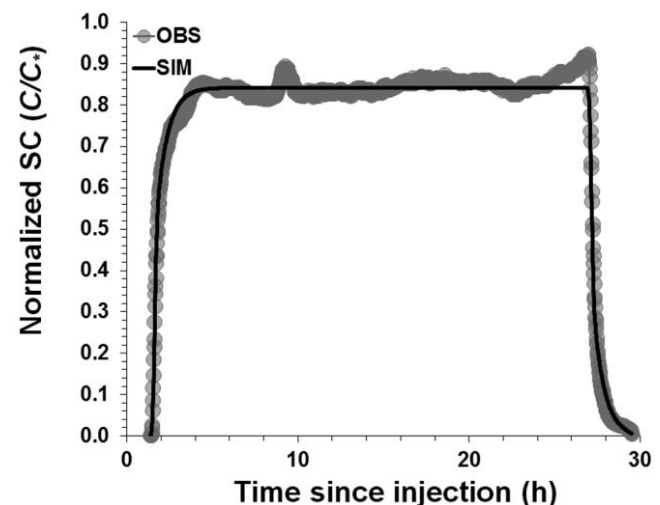

Figure 2. The reach-scale conservative-tracer (specific conductivity [SC]) breakthrough curve (OBS) with the optimal model fit (SIM) for the reach (root mean squared error = 0.02). C = concentration, C_* = peak concentration.

(Table 2). The Experimental Damköhler Number (DaI; Wagner and Harvey 1997) for the reach tracer experiments was 0.37, which is in the ideal range (0.1–1.0) for estimating solute transport and mass transfer parameters.

The stream spiraling analysis of the $^{15}NO_3^-$ addition experiment showed that Drift Creek had a k_{tot} for the reach of 6.0×10^{-4}/m, which results in $S_w = 1667$ m and $V_f = 4.0 \times 10^{-4}$ cm/s (Table 2). k_{den} was 3.3×10^{-4}/m, which is equivalent to 55% of k_{tot}. Reach NO_3^- uptake and denitrification models yielded good simulation fits for observed $^{15}NO_3^-$ dynamics (k_{tot}: $r^2 = 0.89$, Fig. 3; k_{den}: SSE = 1.36, Fig. 4).

Table 2. Multiscale physical transport and NO_3^- reaction parameters for the hyporheic and reach-scale experiments and modeling.

Hyporheic and stream parameters	Abbreviation	Units	Value
Hyporheic zone (HZ) (gravel bar)			
Physical parameters			
Mean residence time	τ_{HZ}	h	14.05
Mass transfer rate	α_{HZ}	/h	0.071
Reaction parameters			
Apparent denitrification rate	k_{HZ}	/h	0.094
NO_3^- uptake rate	λ_{HZ}	/h	0.007
Reach			
Physical parameters			
Mean advection velocity	v	m/h	67.7
Dispersion	D	m^2/h	13.9
Mean storage residence time	τ_{stor}	h	0.49
Mass transfer rate	α_2	/h	2.03
Ratio of storage area to stream area	$\beta_{tot} = A_s/A$	–	0.17
Reaction parameters			
NO_3^- uptake per length	k_{tot}	/m	0.0006
Fractional denitrification rate	k_{den}	/m	0.0003
NO_3^- uptake length	S_w	m	1667
NO_3^- mass-transfer velocity	V_f	cm/s	0.0004
NO_3^- uptake rate	λ_{tot}	/h	0.041
Denitrification rate	λ_{den}	/h	0.022
NO_3^- water-column uptake rate	λ_{stream}	/h	0.034
HZ vs reach			
HZ denitrification proportion of total reach NO_3^- uptake	$\lambda_{HZ}:\lambda_{tot}$	–	0.17
HZ denitrification proportion of total reach denitrification	$\lambda_{HZ}:\lambda_{den}$	–	0.32

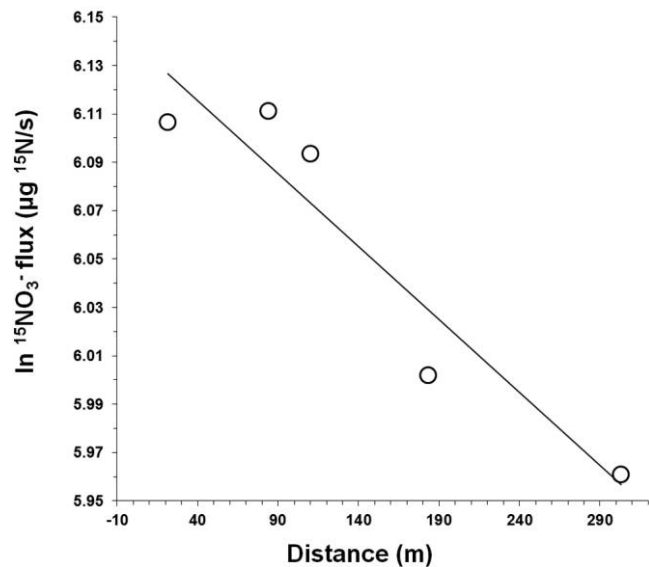Figure 3. The Drift Creek ln($^{15}NO_3^-$ flux) vs distance downstream from the injection site during the steady-state addition experiment. The slope of the regression line is the total fractional NO_3^- uptake rate (k_{tot}), and the negative inverse of the slopes is the NO_3^- uptake length (S_w).

Hyporheic conditions

Repeated measurements of the head elevations in the wells (before plateau sampling disturbances) reflected stable hydraulic head conditions because we detected no variation during the experiment. Solutes advected into the gravel bar with the stream water were altered along the hyporheic flow paths. Mean DO decreased from 8.31 to 0.59 mg O_2/L along HZ flow paths, and the mean DOC decreased from 3.0 to 1.7 mg C/L (Table 1). SUVA$_{254}$ generally decreased along flow paths (3.22–0.94 L mg^{-1} C m^{-1}). The DO and DOC removal rates and $^{15}N_2$ production rates were largest in the first few meters of the flow paths but remained >0 across the entire gravel bar. Overall, NO_3^- decreased along the flow paths from a peak value of 0.54 to 0.02 mg N/L (Fig. 5). The 1st-order NO_3^- removal model (Eq. 3) was able to capture the behavior of the observed hyporheic NO_3^- conditions ($r^2 = 0.83$; Fig. 5) and yielded an apparent 1st-order $k_{HZ} = 0.094$/h (Table 2).

Calculations from the Cl$^-$ breakthrough curves collected at each well showed that median travel times through the HZ ranged from 3.8 to 28.5 h (Table 1). The MODFLOW simulation of hyporheic exchange provided a good fit to observed head (Fig. S1). The simulated head gradients (Fig. 6) and flow paths were generally consistent with the tracer-based median travel times to each of the wells (Table 1, Fig. 7). The flow budget calculations from the groundwater flow model simulation suggested that HEF was 61 L/h at the gravel-bar site, which is equivalent to 4.6% of the
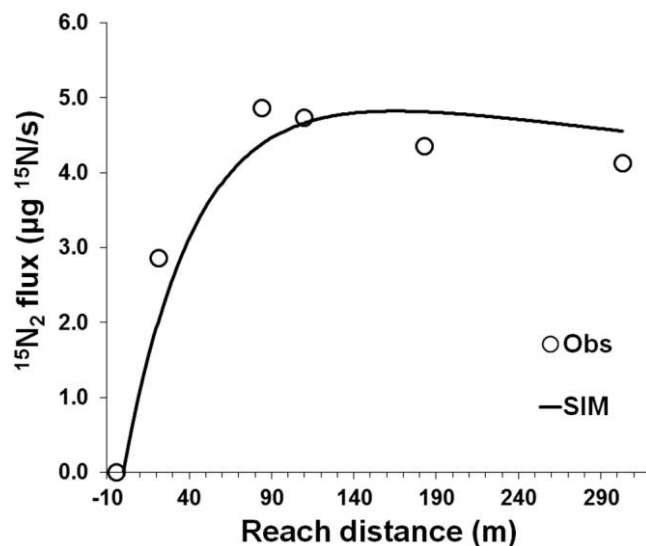
Figure 4. Plot of the $^{15}N_2$ flux vs the distance from the injection site. The solid line shows the best-fit solution of the denitrification simulation (SIM) model to the observed data.

main-channel flow. The mean residence time in the HZ was 14.05 h and α_{HZ} was 0.071/h (Table 2, Fig. 8). The linking of groundwater flow parameters and observed steady-state NO_3^- dynamics resulted in λ_{HZ} = 0.007/h (Table 2).

The ratios of the removal rate pathways for NO_3^- across the reach show that the HZ is responsible for a significant amount of NO_3^- removed from the in-stream water entering the reach. Specifically, the estimated Drift Creek λ_{HZ} accounted for 32% of the total reach denitrification ($\lambda_{HZ}:\lambda_{den}$) and 17% of total reach NO_3^- uptake ($\lambda_{HZ}:\lambda_{tot}$) (Table 2).

DISCUSSION

Interpretations of the HZ NO_3^- removal at the reach scale in this study and similar studies (e.g., Böhlke et al. 2009) must be done cautiously because there are many sources of uncertainty when linking multiscale measurements. Consequently, it is difficult to know if the observed role of the HZ in NO_3^- dynamics in Drift Creek is a true reflection of the physical and biological dynamics of the system or a reflection of the inherent uncertainty associated with making multiscale NO_3^- removal measurements. This same issue was encountered by Böhlke et al. (2009) who synthesized multiscale measurement and modeling (e.g., sediment cores, reach N mass budgets, ^{15}N injections) to assess the role of denitrification in streams. Böhlke et al. (2009) found it very difficult to reconcile and connect the different scales of measurement. Therefore, we discuss the hydroecological processes and methodological issues that control our estimates of hyporheic NO_3^- removal at the reach scale.

Key hydroecological controls on hyporheic NO_3^- removal estimates

The estimated Drift Creek HZ NO_3^- removal rates accounted for 32% of the total reach denitrification and 17% of total reach NO_3^- uptake (Table 2). These removal rates demonstrate that even a volumetrically constrained HZ can control stream NO_3^- during summer baseflow conditions. The estimated importance of hyporheic denitrification at our study site agrees with the synthesis of extensive multiscale investigations conducted in 2 streams of the upper Mississippi River basin. In this synthesis, Böhlke et al. (2009) showed that HZs account for 14 to 97% of the total denitrification occurring at the reach scale. This wide range of HZ denitrification can be attributed to several local hydroecological factors that vary in space and time (Duff and Triska 2000) including, but not limited to, stream flow conditions, amount of hyporheic exchange flow, the water residence times in HZs, the amount of labile DOC available, water temperature, the structure and abundance of hyporheic microbial communities, and the amount of NO_3^- in the system. Each of these factors is expected to be very different between the upper Mississippi River basin and the upper Willamette River basin (our study). Given the limitations of the data at the 2 sites, a comparison among all of these factors is not possible. However, a known key difference is the abundance of NO_3^- in the streams of the 2 basins. The amount of stream NO_3^- in the Böhlke et al. (2009) studies ranged from 1.4 to >14 mg/L, whereas Drift Creek NO_3^- ranges between 0.1 and 0.6 mg/L. The greater availability of NO_3^- in the Mississippi streams alone should result in increased denitrification rates in the HZs that Böhlke et al. (2009) studied
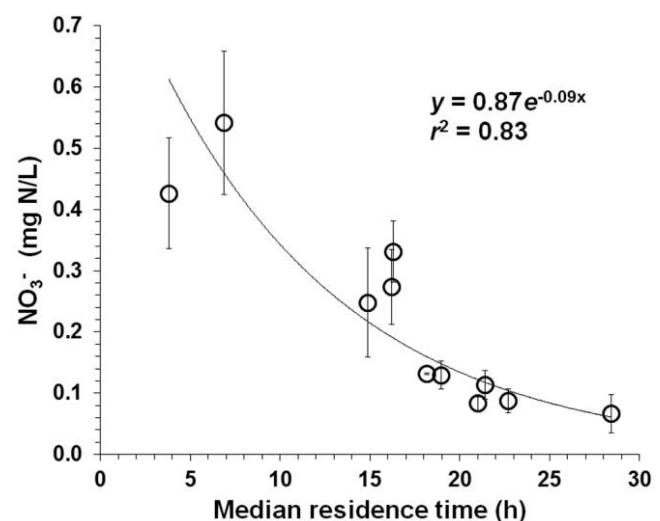

Figure 5. Steady-state hyporheic zone NO_3^- conditions relative to median residence time. Each data point represents the mean (±2 SE) values generated from repeated samples (n = 5) collected during tracer plateau conditions.
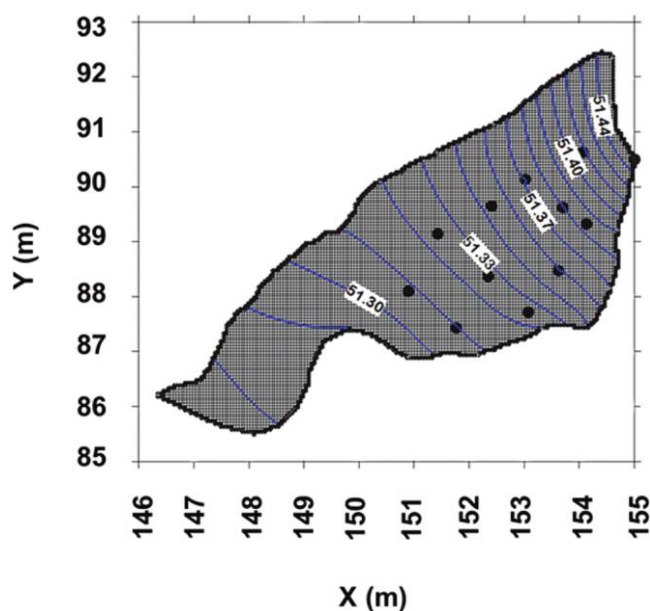
Figure 6. Plan view of the Drift Creek hyporheic exchange model showing the steady-state head gradient across the gravel bar (wells are shown as black circles and the head contours = 0.01 m).

because denitrification rates typically increase with stream NO_3^- availability (Seitzinger 1988, Smith et al. 2006, Mulholland et al. 2008).

The Drift Creek HZ was a net sink for NO_3^- via denitrification (Zarnetske et al. 2011a). However, estimates presented here suggest that the magnitude of this sink is small relative to the NO_3^- flux through the stream channel under baseflow conditions because the HZ within the entire reach removed only 17% of the NO_3^-. That said, substantial sources of uncertainty are associated with these estimates. First, our method combines 1st-order denitrification rate constants measured from long travel-time flow paths (mean $\approx$ 14 h) in our well network with estimates of the relative size of the HZ made from stream-tracer tests, which are insensitive to relatively short residence-time exchange flows (mean = ~0.49 h). The very large changes in DOC, DO, and $^{15}N_2$ between the stream and our first sampling wells (~1 m horizontal distance) suggest that our spatially averaged denitrification rate underestimates the actual rate that should be applied to short residence-time flow paths. Conversely, α_{HZ} is estimated from the MODFLOW simulation of HEF through the gravel bar. Such riffles and gravel bars are relatively common within our study reach, but are not universally distributed. Thus, this exchange parameter probably overestimates the amount of long-residence-time HEF. On the other hand, we did not simulate vertical hyporheic exchange below the wetted stream bed of the riffle where HEF is likely to occur across shorter time scales than through the adjacent gravel bar. Furthermore, β_{tot} is insensitive to the long-residence-time flow

paths, so scaling our estimate of λ_{HZ} by β_{tot} probably results in an underestimate of the actual amount of hyporheic exchange. Taken together, we consider our estimate of the amount of hyporheic denitrification to be conservative in that the sources of uncertainty in our methods are biased toward substantially underestimating whole-reach denitrification.

We observed a large difference between denitrification and total NO_3^- uptake, which probably indicates a large difference in the biological pools using the NO_3^-. Similar results have been reported for other streams. For example, in a 3rd-order, N-limited stream in the nearby Oregon Cascade Mountains, most of the inorganic N uptake occurs in the bryophytes, epixylon, and fine benthic organic material, whereas denitrification was negligible despite the large HZ (Ashkenas et al. 2004). Similarly, the strongly N-limited streams of Antarctica have large hyporheic water flux relative to the main channel, but in these streams most (~74%) of the NO_3^- uptake occurred in the main-channel organisms, whereas the transient-storage zones, including HZs, accounted for the other ~26% (McKnight et al. 2004, Runkel 2007). Background concentrations of dissolved inorganic N are higher in Drift Creek than in the 2 examples cited above, but many biological pools rapidly use and retain the NO_3^- in the reach, as shown by the in-stream uptake rate of 0.034/h. Quantifying the role of each biological pool of N in Drift Creek was not a part of our study, but they seem to be similar to those in the Cascade and Antarctic N-limited streams in that in-stream NO_3^- retention and removal is important to reach-scale NO_3^- uptake. Furthermore, denitrification accounted for only 16% of the total reach-scale NO_3^- uptake, on average, across all the North American LINX2 study sites (Mulholland et al. 2008). Thus, our results are in line with this relatively small role of denitrification on overall NO_3^- uptake seen across a wide range of streams.

Biogeochemical and physical limitations on hyporheic denitrification exist in Drift Creek. Zarnetske et al. (2011b) showed that the availability of labile DOC limited hyporheic denitrification ($SUVA_{254}$ decreased along flow paths; Table 1). The physical size of the HZ also probably limited hyporheic denitrification. The stream is channelized in our experimental reach so that alluvial sediment in the active channel ranges in depth from 0 to 1.5 m, which constrains the volume of sediment where NO_3^- removal can occur. Both factors limit the influence of the hyporheic exchange at the reach scale (Zarnetske et al. 2008, Tonina and Buffington 2011).

Key methodological limitations on hyporheic NO_3^- removal estimates

We chose to use an experimental approach that allowed us to examine the influence of hyporheic processes throughout many cubic meters of sediment in which we
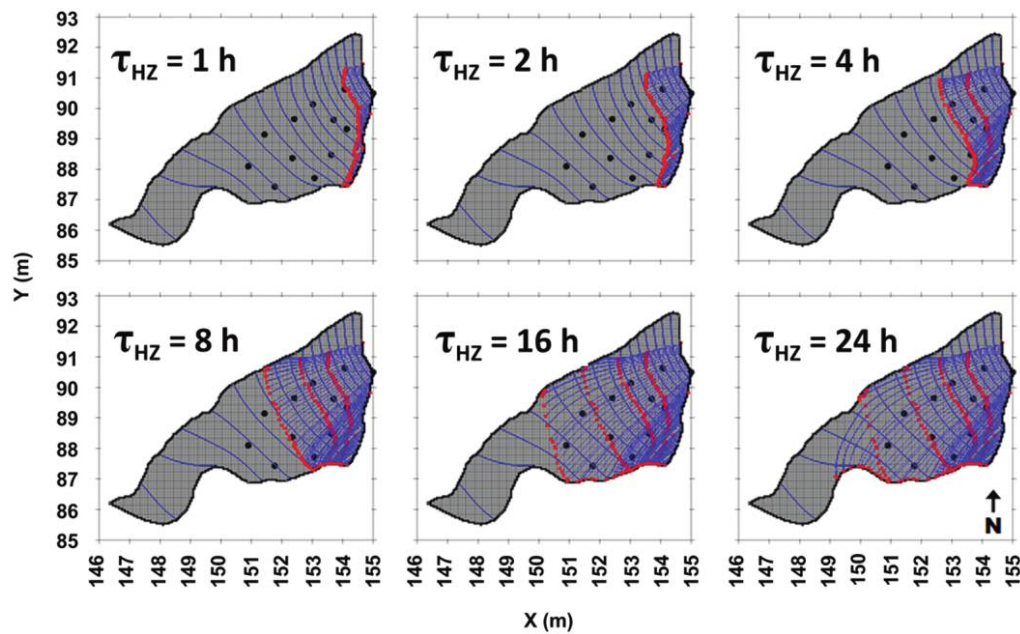
Figure 7. Hyporheic flowpath simulations for different residence times (τ_{HZ}) in the Drift Creek hyporheic zone (HZ). Flow paths are shown in blue with the residence-time-defined termination point shown as a red circle.

maintained minimally disturbed conditions. This approach enabled us to study in-situ N transformations and allowed us to make an integrated and robust measurement of natural hyporheic processes at the scale of our gravel bar (~10 m). However, it presented problems when upscaling these processes to explain the role of the HZ at the whole reach (~300 m).

We used reach-scale ^{15}N tracer experiments to measure NO_3^- removal and denitrification rates because the ^{15}N-tracer method is a robust and commonly used measurement technique. The strength of using ^{15}N additions in an NO_3^--removal experiment is that one can follow the ^{15}N in the $^{15}NO_3^-$ molecules through a system, including the denitrification pathway via $^{15}N_2$ production, while minimally altering the ambient NO_3^- conditions in the ecosystem (Mulholland et al. 2004, 2008). However, the method has many sources of uncertainty. One key source of uncertainty that is not specific to hyporheic investigations is estimation of gas-transfer rates between stream and atmosphere (reaeration) (Wallin et al. 2011). This rate is an important parameter of the Mulholland et al. (2004) methods and affects the calculated reach denitrification of our study and other similar studies that depend on transfer rates of dissolved gases (e.g., metabolism). Wallin et al. (2011) showed that general models, such as that of Owens (1974), can have large errors in estimates of reaeration. New scaling equations for reaeration in streams based on channel geometry and hydraulics, including N_2, have been developed since we completed our study (e.g., Raymond et al. 2012), and may offer better ways to account for these processes indirectly when estimating denitrification. Nev-

ertheless, we suggest that more accurate direct measurements of gas exchange (e.g., SF_6 or propane tracing) should be done for future process-based studies of stream and hyporheic denitrification, especially in streams with steep longitudinal gradients or high flow velocities, where new scaling methods, such as that of Raymond et al. (2012), may be less accurate.

Another key source of uncertainty in the $^{15}NO_3^-$ tracer method is associated with the measurements of the physical transport conditions needed to estimate NO_3^- uptake and denitrification (Böhlke et al. 2009). Böhlke et al. (2009), like most investigators of $^{15}NO_3^-$ uptake, calculated their physical transport parameters, including the apparent hyporheic–surface-water transport parameters (A_s and α) from a reach-scale 1D solute-transport model (e.g., OTIS; Runkel et al. 1998). In contrast, we quantified the actual hyporheic exchange flow (Q_{HEF}) and the mass exchange rates (α_{HZ}) for our gravel bar, rather than relying on a single α determined from a reach-scale transient-storage model. However, to link and scale our hyporheic measurements up to the reach-scale processes, we had to assume that the apparent mean denitrification rate measured in our gravel-bar study site was representative of hyporheic processes occurring throughout the entire reach. We deliberately focused our research on an exposed, unvegetated gravel bar between the wetted edge of the stream and the channelized bankfull channel. The gravel bar was easily accessible, and, although parafluvial in nature, we expected that the saturated alluvium beneath the surface of the gravel bar would not be fundamentally different from the alluvium throughout the rest of our study reach.
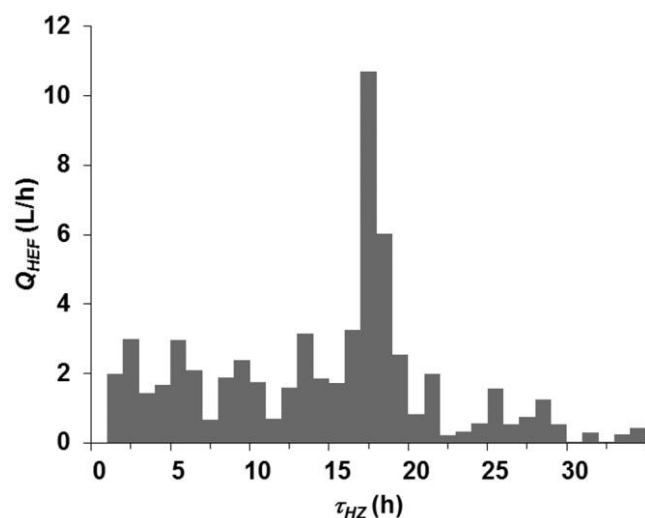
Figure 8. The distribution of hyporheic exchange flow (Q_{HEF}) across the hyporheic residence times (τ_{HZ}) in the experimental gravel-bar site.

Furthermore, the channel bank and substrate beneath the accumulated alluvium was fine textured and, thus, provided a clearly bounded system in which we could carefully observe hyporheic exchange flows with a wide range of residence times and biogeochemical gradients. The flow paths were arrayed laterally, which allowed us to more accurately isolate different residence times along the length of the gravel bar rather than attempting to distinguish and sample different residence times from vertically nested hyporheic flow paths under the thalweg or those that occur over very small flowpath lengths (< cm scale). Thus, we were able to reduce the uncertainty in our estimates by measuring distinct flow paths with clear biogeochemical gradients and then use these measurements to estimate representative biogeochemical rates from which we could scale results measured at the scale of the gravel bar to the full stream reach.

Reasonable alternative approaches do exist for linking rate constants for biogeochemical processes to reach-scale physical-transport parameters. For example, a study scheme could be designed with intensive sampling throughout the reach to measure physical and biogeochemical processes relevant to denitrification in an attempt to characterize the broad range of variability in HZ processes within the reach. However, the tools and techniques would be very different from those we used, and such a distributed approach would introduce different sources of error and uncertainty that also would make scaling hyporheic function up to the reach difficult. Below, we discuss the key sources of uncertainty inherent to our method of linking the gravel-bar-scale characterizations to the reach-scale-based characterizations of denitrification.

Hyporheic residence times are a key factor determining the effectiveness of the HZ as a sink of NO_3^- to the stream (Zarnetske et al. 2011a, 2012), and these residence times typically range across orders of magnitude in any given stream. In Drift Creek, we observed coupled nitrification and denitrification in locations with hyporheic residence times <6.9 h during the 2007 baseflow conditions, whereas denitrification was dominant at locations with longer residence times. However, the overall effect of N cycling on a stream must balance the influence of residence time with the amount of HEF and the rate of denitrification. For example, Harvey et al. (2013) demonstrated that the locations having the greatest influence on total reach-scale denitrification did not occur in areas with the longest residence times or with the highest through-put of HEF. Rather, in their low-gradient, sand-bedded stream, the vertical exchange flows along 2- to 6-cm flow paths in low-energy channel side-cavity environments had residence times of minutes and had the largest influence because these locations were able to maintain moderate levels of HEF and very high reaction rates. Slightly longer vertical flow paths of ∼18 cm in the same stream had much longer residence times (up to 88 h) and a weak influence on overall denitrification because these locations had low HEF and reaction substrate limitations.

Differences between the observed and measured residence-time distributions of hyporheic exchange can greatly influence estimates of the relative magnitude of denitrification. For example, if the whole-reach measured residence-time distribution had been heavily biased toward the very shortest residence-time flow paths in the Drift Creek HZ (i.e., submeter flow paths with seconds to minutes for residence times), we would have underestimated the importance of hyporheic denitrification by mischaracterizing much of the denitrification occurring within reaction sites of the active stream channel. Conversely, if the hyporheic-flow-weighted residence-time distribution had been heavily skewed toward longer residence-time flow paths than those detected by the in-stream tracers, we would have simply underestimated the total amount of hyporheic denitrification because exchange flows at long time scales would not have been observed in our whole-reach tracer experiment. This 'window of detection' issue (Wagner and Harvey 1997, Harvey and Wagner 2000) is discussed further below.

Last, our method for quantifying the role of the HZ on whole-stream NO_3^- uptake and denitrification is based on simple advection-based models of hyporheic exchange, which do not account for the diffusion-dominated microscale (μm–cm scale) or the complexities of dual-domain mass transfer (e.g., Harvey et al. 1994, Haggerty and Gorelick 1995). The microscale domain is where stream water interacts with denitrifying biofilms coating the sediment of the stream bed (Sørensen et al. 1988) and can create biogeochemical hotspots (Hill et al. 1998, McClain et al. 2003). If such microsites are prevalent along the stream–hyporheic interface, as indicated by previous stud-

ies (Holmes et al. 1996, Zarnetske et al. 2011a, Harvey et al. 2013), they could be important locations for additional denitrification that were not accounted for in our modeling approach. Collectively, these sources of underestimation indicate that the HZ may play a larger role in reach-scale denitrification in Drift Creek than our methods reveal and may help explain why other reach-scale–based estimates of hyporheic residence time and denitrification are consistently characterized as a small portion of total NO_3^- uptake.

Uncertainty in estimates of hydrologic conditions also is associated with the window of detection for reach-scale tracer experiments (Wagner and Harvey 1997, Harvey and Wagner 2000). The window of detection of reach-tracer experiments may render tracers that enter long-residence-time pathways, such as hyporheic flow paths, undetectable. Consequently, the subsequent transport modeling of the stream-tracer dynamics (e.g., Stream Solute Workshop 1990) may not be sensitive to the long exchange time scales and much of the hyporheic volume. This means that reach tracer tests typically underestimate the volume of the transient-storage zone, including the HZ, and also underestimate hyporheic exchange occurring at long time scales. This underestimation of exchange time scales by stream tracers was recently observed during a comparison of physically based stream–groundwater models to results of stream tracer experiments (Stonedahl et al. 2012) and is a source of uncertainty for any study based on reach-scale tracer methods.

Inspection of the modeled Drift Creek gravel-bar HZ residence times and the reach-scale mean residence time in Drift Creek indicate a window of detection problem in our study despite a good *DaI* (Wagner and Harvey 1997) because they are very different (τ_{HZ} = 14.05 h vs τ_{stor} = 0.49 h). This difference indicates that the reach-scale methods at Drift Creek may not have detected much of the hyporheic NO_3^--transformation processes because they operated over time scales much longer than that of the observed reach transport time scales. Approximately 11% of the hyporheic flow occurs at time scales longer than the time scales of the ^{15}N plateau sampling period used to calculate the λ_{tot} and λ_{den} (i.e., 22.5–27.5 h after start of injection) (Fig. 8). Thus, even though we sampled at tracer plateau conditions, ~11% of the hyporheic flow paths had not yet returned to the main channel and, therefore, would not have influenced the reach-scale measurements. In terms of spatial scales, inspection of Eq. 5 shows that λ_{HZ} is very sensitive (i.e., directly proportional) to the reach measured β_{tot}, and the Q_{HEF} time scales demonstrate that the reach-scale tracer experiments are insensitive to the full residence-time distribution of hyporheic exchange flows. Therefore, the apparent λ_{HZ} probably is an underestimate of the true λ_{HZ} in Drift Creek. Zarnetske et al. (2011a) showed net denitrification rates occurring over time scales >6.9 h in the Drift Creek HZ during summer base flow,

so the ~11% of Q_{HEF} not observed during the main-channel plateau sampling was dominated by strong denitrification potentials that were not realized by the reach-scale estimates of denitrification.

Overall, the limitations imposed by the windows of detection on reach-scale tracer experiments create experimental artifacts that lead to systematic underestimation of the influence of transient storage on stream biogeochemical cycles. These transient-storage zones include both surface-channel features and HZs that are typically among the most biogeochemically reactive environments in streams (Baker et al. 2000, McClain et al. 2003, Harvey et al. 2013). As a result, methods of characterizing hyporheic biogeochemical function that are based on current reach-scale tracer measurements and models may be unable to characterize the very rapid and very long hyporheic time-scale processes, a situation that limits our ability to use these methods to scale processes like hyporheic denitrification to entire stream reaches or the stream network.

Researchers (e.g., Stonedahl et al. 2012, Harvey et al. 2013, Ward et al. 2014, this study) are starting to converge on new ways to address the window-of-detection issue in hyporheic studies. We suggest that researchers make many direct measurements of residence times that are spatially distributed throughout the reach and are designed to sample as many stream and hyporheic transient-storage compartments as possible. Given such data, it should become possible to relate the time scales of transient storage measured in whole-reach studies to the specific stream and hyporheic environments that are influential at those time scales and, thereby, to improve our interpretation of tracer studies. In our study, direct measurements of hyporheic transient-storage dynamics from our well network provided us with a way to link empirically derived reach-scale measurement of overall transient-storage-zone size and mass-exchange rates with direct hyporheic transient-storage-zone measurements and models of residence times and mass-exchange rates. Thus, we are moving toward bridging the time-scale gaps between methods. If investigators interested in quantifying the role of transient-storage zones in streams make efforts to characterize key physical- and biological-process time scales of transient-zone compartments, such as the HZ in our study, they will be able to quantify the differences in residence-time scales between the in-stream and transient-storage zones and use that information to better interpret their reach-scale tracer results.

Conclusions

We used independent and complementary methods to estimate of HZ denitrification at the reach scale in situ at summer base flow. We estimated that the HZ accounted for 17% of the total reach NO_3^- uptake and 32% of the total reach denitrification. These results emphasize the potential role of the HZ as a regulator of aquatic N

dynamics, but they also highlight many methodological limitations that introduce uncertainty to these estimates of N removal. The methods that integrate biogeochemical reaction kinetics with physical transport kinetics at the reach scale present multiple sources of bias that lead to underestimation of hyporheic denitrification detected by reach-scale tracer experiments. The primary source of bias identified in our study was the window-of-detection issue of reach-scale tracer tests, which limits our ability to characterize the very rapid and very long hyporheic time-scale processes. Therefore, additional HZ characterizations are necessary and worth the effort when trying to link hyporheic and in-stream processes. For example, we collected many in-situ measurements and used process-based models to identify transport and reaction time scales within the HZ. This HZ time-scale information greatly informed the quantification and interpretation of the reach-scale NO_3^- uptake study. This additional hyporheic information, or similar information, will aid future investigators in their interpretations of reach-scale characterizations and help reduce uncertainty when identifying controlling processes, such as the role of hyporheic denitrification at the river reach and network scales. Therefore, developing new methods and frameworks that aid in the collection and linking of multiscale hydrologic and ecological data is a grand and exciting challenge for the stream ecology and hyporheic research community.

LITERATURE CITED

→ Argerich, A., R. Haggerty, E. Martí, F. Sabater, and J. P. Zarnetske. 2011. Quantification of metabolically active transient storage (MATS) in two reaches with contrasting transient storage and ecosystem respiration. Journal of Geophysical Research 116:G03034.

→ Ashkenas, L. R., S. L. Johnson, S. V. Gregory, J. L. Tank, and W. M. Wollheim. 2004. A stable isotope tracer study of nitrogen uptake and transformation in an old-growth forest stream. Ecology 85:1725–1739.

→ Baker, M. A., C. N. Dahm, and H. M. Valett. 1999. Acetate retention and metabolism in the hyporheic zone of a mountain stream. Limnology and Oceanography 44:1530–1539.

→ Baker, M. A., H. M. Valett, and C. N. Dahm. 2000. Organic carbon supply and metabolism in a shallow groundwater ecosystem. Ecology 81:3133–3148.

Bard, Y. 1974. Nonlinear parameter estimation. Academic Press, San Diego, California.

→ Beaulieu, J. J., J. L. Tank, S. K. Hamilton, W. M. Wollheim, R. O. Hall, P. J. Mulholland, B. J. Peterson, L. R. Ashkenas, L. W. Cooper, C. N. Dahm, W. K. Dodds, N. B. Grimm, S. L. Johnson, W. H. McDowell, G. C. Poole, H. M. Valett, C. P. Arango, M. J. Bernot, A. J. Burgin, C. L. Crenshaw, A. M. Helton, L. T. Johnson, J. M. O'Brien, J. D. Potter, R. W. Sheibley, D. J. Sobota, and S. M. Thomas. 2011. Nitrous oxide emission from denitrification in stream and river networks. Proceedings of the National Academy of Sciences of the United States of America 108:214–219.

→ Bencala, K. E., and R. A. Walters. 1983. Simulation of solute transport in a mountain pool-and-riffle stream: a transient storage model. Water Resources Research 19:718–724.

→ Birgand, F., R. W. Skaggs, G. M. Chescheir, and J. W. Gilliam. 2007. Nitrogen removal in streams of agricultural catchments—a literature review. Critical Reviews in Environmental Science and Technology 37:381–487.

→ Böhlke, J. K., R. C. Antweiler, J. W. Harvey, R. L. Smith, M. A. Voytek, A. Laursen, L. K. Smith. 2009. Multi-scale measurements and modeling of denitrification in streams with varying flow and nitrate concentration in the upper Mississippi River basin, USA. Biogeochemistry 93:117–141.

Botter, G., N. B. Basu, S. Zanardo, P. S. C. Rao, and A. Rinaldo. 2010. Stochastic modeling of nutrient losses in streams: interactions of climatic, hydrologic, and biogeochemical controls. Water Resources Research 46. doi:10.1029/2009WR008758

→ Bouwer, H., and R. C. Rice. 1976. A slug test method for determining hydraulic conductivity of unconfined aquifers with completely or partially penetrating wells. Water Resources Research 12:423–428.

→ Boyer, E. W., R. B. Alexander, W. J. Parton, C. Li, K. Butterbach-Bahl, S. D. Donner, R. W. Skaggs, and S. J. Del Grosso. 2006. Modeling denitrification in terrestrial and aquatic ecosystems at regional scales. Ecological Applications 16:2123–2142.

→ Diaz, R. J., and R. Rosenberg. 2008. Spreading dead zones and consequences for marine ecosystems. Science 321:926–929.

Duff, J. H., and F. J. Triska. 2000. Nitrogen biogeochemistry and surface–subsurface exchange in streams. Pages 197–217 *in* J. A. Jones and P. J. Mulholland (editors). Streams and ground waters. Academic Press, San Diego, California.

Freeze, R., and J. Cherry. 1979. Groundwater. Prentice–Hall, Upper Saddle River, New Jersey.

→ Groffman, P. M., M. A. Altabet, J. K. Böhlke, K. Butterbach-Bahl, M. B. David, M. K. Firestone, A. E. Giblin, T. M. Kana, L. P. Nielsen, and M. A. Voytek. 2006. Methods for measur-

ing denitrification: diverse approaches to a difficult problem. Ecological Applications 16:2091–2122.

→ Gruber, N., and J. N. Galloway. 2008. An Earth-system perspective of the global nitrogen cycle. Nature 451:293–296.

→ Haggerty, R., and S. M. Gorelick. 1995. Multiple-rate mass transfer for modeling diffusion and surface reactions in media with pore-scale heterogeneity. Water Resources Research 31:2383–2400.

Haggerty, R., and P. C. Reeves. 2002. STAMMT-L version 1.0 user's manual. ERMS 520308. Sandia National Laboratories, Albuquerque, New Mexico.

→ Haggerty, R., S. M. Wondzell, and M. A. Johnson. 2002. Power-law residence time distribution in the hyporheic zone of a 2nd-order mountain stream. Geophysical Research Letters 29:1640.

→ Harvey, J. W., J. K. Böhlke, M. Voytek, D. Scott, and C. R. Tobias. 2013. Hyporheic zone denitrification: controls on effective reaction depth and contribution to whole-stream mass balance. Water Resources Research 49:6298–6316.

→ Harvey, C. F., R. Haggerty, and S. M. Gorelick. 1994. Aquifer remediation: a method for estimating mass transfer rate coefficients and an evaluation of pulsed pumping. Water Resources Research 30:1979–1991.

Harvey, J. W., and B. J. Wagner. 2000. Quantifying hydrologic interactions between streams and their subsurface hyporheic zones. Pages 3–44 in J. A. Jones and P. J. Mulholland (editors). Streams and ground waters. Academic Press, San Diego, California.

→ Hedin, L. O., J. C. von Fischer, N. E. Ostrom, B. P. Kennedy, M. G. Brown, and G. P. Robertson. 1998. Thermodynamic constraints on nitrogen transformations and other biogeochemical processes at soil–stream interfaces. Ecology 79:684–703.

→ Hill, A. R., C. F. Labadia, and K. Sanmugadas. 1998. Hyporheic zone hydrology and nitrogen dynamics in relation to the streambed topography of a N-rich stream. Biogeochemistry 42:285–310.

→ Holmes, R. M., J. B. Jones, S. G. Fisher, and N. B. Grimm. 1996. Denitrification in a nitrogen-limited stream ecosystem. Biogeochemistry 33:125–146.

→ Kasahara, T., and S. M. Wondzell. 2003. Geomorphic controls on hyporheic exchange flow in mountain streams. Water Resources Research 39:1005.

→ Marquardt, D. W. 1963. An algorithm for least-squares estimation of nonlinear parameters. Journal of the Society for Industrial and Applied Mathematics 11:431–441.

Marzadri, A., D. Tonina, and A. Bellin. 2012. Morphodynamic controls on redox conditions and on nitrogen dynamics within the hyporheic zone: application to gravel-bed rivers with alternate-bar morphology. Journal of Geophysical Research 117. doi:10.1029/2012JG001966

→ McClain, M. E., E. W. Boyer, C. L. Dent, S. E. Gergel, N. B. Grimm, P. M. Groffman, S. C. Hart, J. W. Harvey, C. A. Johnston, E. Mayorga, W. H. McDowell, and G. Pinay. 2003. Biogeochemical hot spots and hot moments at the interface of terrestrial and aquatic ecosystems. Ecosystems 6:301–312.

→ McKnight, D. M., R. L. Runkel, C. M. Tate, J. H. Duff, and D. L. Moorhead. 2004. Inorganic N and P dynamics of Antarctic glacial meltwater streams as controlled by hyporheic exchange and benthic autotrophic communities. Journal of the North American Benthological Society 23:171–188.

→ Mulholland, P. J., A. M. Helton, G. C. Poole, R. O. Hall, S. K. Hamilton, B. J. Peterson, J. L. Tank, L. R. Ashkenas, L. W. Cooper, C. N. Dahm, W. K. Dodds, S. E. G. Findlay, S. V. Gregory, N. B. Grimm, S. L. Johnson, W. H. McDowell, J. L. Meyer, H. M. Valett, J. R. Webster, C. P. Arango, J. J. Beaulieu, M. J. Bernot, A. J. Burgin, C. L. Crenshaw, L. T. Johnson, B. R. Niederlehner, J. M. O'Brien, J. D. Potter, R. W. Sheibley, D. J. Sobota, and S. M. Thomas. 2008. Stream denitrification across biomes and its response to anthropogenic nitrate loading. Nature 452:202–205.

→ Mulholland, P. J., H. M. Valett, J. R. Webster, S. A. Thomas, L. W. Cooper, S. K. Hamilton, and B. J. Peterson. 2004. Stream denitrification and total nitrate uptake rates measured using a field ^{15}N tracer addition approach. Limnology and Oceanography 49:809–820.

→ Newbold, J. D., J. W. Elwood, R. V. O'Neill, and W. Van Winkle. 1981. Measuring nutrient spiralling in streams. Canadian Journal of Fisheries and Aquatic Sciences 38:860–863.

Owens, M. 1974. Measurements on non-isolated natural communities in running waters. Pages 111–119 in R. A. Vollenweider (editor). A manual on methods for measuring primary production in aquatic environments. Blackwell Scientific Publications, Oxford, UK.

→ Peterson, B. J., W. M. Wollheim, P. J. Mulholland, J. R. Webster, J. L. Meyer, J. L. Tank, E. Martí, W. B. Bowden, H. M. Valett, A. E. Hershey, W. H. McDowell, W. K. Dodds, S. K. Hamilton, S. Gregory, and D. D. Morrall. 2001. Control of nitrogen export from watersheds by headwater streams. Science 292:86–90.

→ Raymond, P. A., C. J. Zappa, D. Butman, T. L. Bott, J. Potter, P. Mulholland, A. E. Laursen, W. H. McDowell, and D. Newbold. 2012. Scaling the gas transfer velocity and hydraulic geometry in streams and small rivers. Limnology and Oceanography: Fluids and Environments 2:41–53.

→ Runkel, R. L. 2007. Toward a transport-based analysis of nutrient spiraling and uptake in streams. Limnology and Oceanography: Methods 5:50–62.

→ Runkel, R. L., D. M. McKnight, and E. D. Andrews. 1998. Analysis of transient storage subject to unsteady flow: diel flow variation in an Antarctic stream. Journal of the North American Benthological Society 17:143–154.

→ Sala, O. E., F. S. Chapin, J. J. Armesto, E. Berlow, J. Bloomfield, R. Dirzo, E. Huber-Sanwald, L. F. Huenneke, R. B. Jackson, A. Kinzig, R. Leemans, D. M. Lodge, H. A. Mooney, M. Oesterheld, N. L. Poff, M. T. Sykes, B. H. Walker, M. Walker, and D. H. Wall. 2000. Global biodiversity scenarios for the year 2100. Science 287:1770–1774.

→ Seitzinger, S., J. A. Harrison, J. K. Böhlke, A. F. Bouwman, R. Lowrance, B. Peterson, C. Tobias, and G. Van Drecht. 2006. Denitrification across landscapes and waterscapes: a synthesis. Ecological Applications 16:2064–2090.

→ Seitzinger, S. P. 1988. Denitrification in freshwater and coastal marine ecosystems: ecological and geochemical significance. Limnology and Oceanography 33:702–724.

→ Seitzinger, S. P., and C. Kroeze. 1998. Global distribution of nitrous oxide production and N inputs in freshwater and coastal marine ecosystems. Global Biogeochemical Cycles 12:93–113.

→ Smith, L. K., M. A. Voytek, J. K. Böhlke, and J. W. Harvey. 2006. Denitrification in nitrate-rich streams: application of N_2:Ar and N^{15}-tracer methods in intact cores. Ecological Applications 16:2191–2207.

→ Smith, V. H. 2003. Eutrophication of freshwater and coastal marine ecosystems—a global problem. Environmental Science and Pollution Research 10:126–139.

→ Sørensen, J., T. Jorgensen, and S. Brandt. 1988. Denitrification in stream epilithon—seasonal variation in Gelbaek and Rabis-Baek, Denmark. FEMS Microbiology Ecology 53:345–354.

→ Stonedahl, S. H., J. W. Harvey, J. Detty, A. Aubeneau, and A. I. Packman. 2012. Physical controls and predictability of stream hyporheic flow evaluated with a multiscale model. Water Resources Research 48:W10513.

→ Stream Solute Workshop. 1990. Concepts and methods for assessing solute dynamics in stream ecosystems. Journal of the North American Benthological Society 9:95–119.

→ Tonina, D., and J. M. Buffington. 2011. Effects of stream discharge, alluvial depth and bar amplitude on hyporheic flow in pool-riffle channels. Water Resources Research 47:08508.

→ Valett, H. M., J. A. Morrice, C. N. Dahm, and M. E. Campana. 1996. Parent lithology, surface–groundwater exchange, and nitrate retention in headwater streams. Limnology and Oceanography 41:333–345.

→ Wagner, B. J., and J. W. Harvey. 1997. Experimental design for estimating parameters of rate-limited mass transfer: analysis of stream tracer studies. Water Resources Research 33:1731–1741.

Wallin, M. B., M. G. Oquist, I. Buffam, M. F. Billett, J. Nisell, and K. H. Bishop. 2011. Spatiotemporal variability of the gas transfer coefficient (kCO_2) in boreal streams: implications for large scale estimates of CO_2 evasion. Global Biogeochemical Cycles 25:GB3025.

→ Ward, A. S., M. N. Gooseff, M. Fitzgerald, T. J. Voltz, and K. Singha. 2014. Spatially distributed characterization of hyporheic solute transport during baseflow recession in a headwater mountain stream using electrical geophysical imaging. Journal of Hydrology 517:362–377.

→ Webster, J. R., and B. C. Patten. 1979. Effects of watershed perturbation on stream potassium and calcium dynamics. Ecological Monographs 49:51–72.

Webster, J. W., and H. M. Valett. 2006. Pages 169–186 *in* F. R. Hauer, and G. A. Lamberti (editors). Methods in stream ecology. Elsevier, New York.

→ Wondzell, S. M., J. LaNier, and R. Haggerty. 2009. Evaluation of alternative groundwater flow models for simulating hyporheic exchange in a small mountain stream. Journal of Hydrology 364:142–151.

→ Zarnetske, J. P., M. N. Gooseff, W. B. Bowden, M. J. Greenwald, J. P. McNamara, J. H. Bradford, and T. R. Brosten. 2008. Influence of morphology and permafrost dynamics on hyporheic exchange in arctic headwater streams under warming climate conditions. Geophysical Research Letters 35:L02501.

→ Zarnetske, J. P., R. Haggerty, S. M. Wondzell, and M. A. Baker. 2011a. Dynamics of nitrate production and removal as a function of residence time in the hyporheic zone. Journal of Geophysical Research 116:G01025.

→ Zarnetske, J. P., R. Haggerty, S. M. Wondzell, and M. A. Baker. 2011b. Labile dissolved organic carbon supply limits hyporheic denitrification. Journal of Geophysical Research 116:G04036.

Zarnetske, J. P., R. Haggerty, S. M. Wondzell, V. Bokil, and R. González-Pinzón. 2012. Coupled transport and reaction kinetics control the nitrate source-sink function of hyporheic zones. Water Resources Research 48:W11508.